Characterization of a fiber laser system for materials processing

Author: Pol Paniagua Seriols.
Advisor: Juan Marcos Fernández
Facultat de Física, Universitat de Barcelona, Diagonal 645, 08028 Barcelona, Spain*.

Abstract: The physical parameters of the emission of a commercial Q-switched, Yb doped, 20 W fiber laser were measured and analysed under different operating conditions. The laser showed a gaussian profile, and its diameter and peak power coincided with the specifications, but the maximum beam power and pulse energies were 16% lower. The beam power correlated linearly with the pump power. The pulse energy increases with the pulse length for 2 and 20 kHz repetition rates but a ceiling of 80 μJ is attained for 200 kHz. The time needed to attain the maximum population inversion is about 50 μs. The time shape of the pulses is strongly dependent on the pulse length and changes significantly when going from 2 and 20 kHz to 200 kHz, probably due to the low population inversion attained in the latter case.

I. INTRODUCTION

Lasers have become ubiquitous in science and technology. Although the first working laser had a ruby crystal as gain medium [1], the use of a glass fiber for this purpose was proposed and implemented very shortly after [2-4]. However, fiber media were not fully developed until the 1990s, when the diode-pumping technology was developed [5]. Fiber lasers compete favourably with traditional lasers in robustness, stability, efficiency, compact size and optical quality, making them especially suitable for certain applications, such as telecommunications, materials processing and medicine. In most cases the fiber is a silica glass doped with rare-earth atoms such as ytterbium (Yb), erbium, neodymium, thulium, praseodymium or holmium [6]. These elements have absorption/emission bands ranging from de near-infrared to the ultraviolet, which allows to design lasers working in a wide spectrum of wavelengths. The fiber is usually embedded inside a cladding made of a material with lower refraction index, so that total internal reflection keeps the radiation inside the fiber even for curved geometries. Hence, the focusing element can be movable, which is important in certain cutting, welding, and folding applications. Also, they can be very long (up to the kilometre range) which provides a high optical gain. Output powers from less than 1 mW to tens of kW can be achieved [7]. The large area to volume ratio allows efficient cooling, and if the fiber is thin enough, single-mode radiation is produced. The pump source is usually another laser, typically a diode laser.

The goal of the present work is to gain a better knowledge of the physical parameters of the emission of a commercial Yb-doped fiber laser through the measurement and analysis of the pulse features under different operating conditions.

II. EXPERIMENTAL

A. Laser features

The laser used was a Powerline F20 Varia from the manufacturer Coherent Rofin [8]. It is an air-cooled, diode-pumped, Q-switched pulsed laser. The fiber is doped with ytterbium (Yb), and the operating wavelength is 1064 nm, lying in the near infrared. The Yb^{3+} ions have a very simple energy-level structure (see Fig. 1) with no excited states absorbing at either pump or laser wavelengths, which allows 4-level lasing with high efficiency [9, 10]. Pulse repetition rates from 2 to 1000 kHz, and the pulse lengths from 4 to 200 ns can be selected.
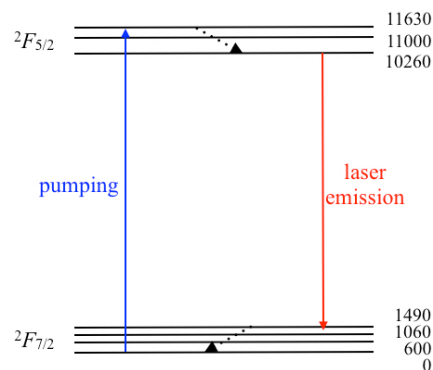

FIG. 1: Energy levels in cm^{-1} and transitions involved in the operation of a Yb-doped fiber laser.

According to the manufacturer specifications [11] the average beam power is 19 W and the energy of a 200 ns pulse is 0.95 mJ with a peak power of 10 kW at a repetition rate of 20 kHz. The beam diameter at the output is 5.0±1.0 mm, and the divergence is ±0.5 mrad. The beam quality as measured by the M^2 index is <2.0. An alignment visible laser of <1 mW working at 600-700 nm is included. A marker head is provided that allows working on a 120×120 mm^2 area. It contains two mirrors that deviate the beam emitted by the laser in the x and y axes before it is focused on the working surface with a lens of f=100 mm (the "galvo" system). The different parts of the laser are assembled as shown in Fig. 2. The whole system is controlled by a personal computer.

The main use of this laser is high-speed and high-precision marking of metallic or polymer materials.
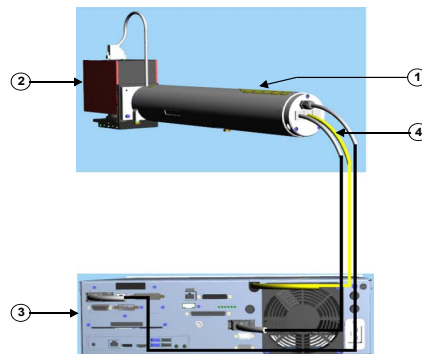

FIG. 2: Laser system: 1) Laser head. 2) Marking head. 3) Plug-in supply unit. 4) Transport fiber. Figure taken from reference [11].

_____

* Electronic address:ppaniase7@alumnes.ub.edu

B. Experimental setup

Two main types of simultaneous measurements were performed:

- the average power of the laser beam was measured with a thermopile sensor,
- the instantaneous radiation power at very small time-increments were measured with a photodiode.

To perform such measurements the light emitted by the laser was focused downwards to a low-reflectance glass oriented at an angle of 45º with respect to the beam (see Fig. 3). This creates two beams: one went through the glass to the thermopile, and the reflected one met the photodiode. The low-reflectance glass was near the lens focus (10 cm), and the measuring instruments were set at roughly 22 cm from the lens to prevent any possible damage. The photodiode was somewhat separated from the centre of the beam to avoid saturation.
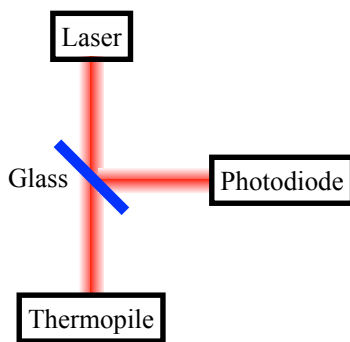

FIG. 3: Scheme of the experimental setup.

The thermopile was connected to a voltmeter, giving a lecture that was taken manually. Two different thermopiles were used. A small one reaching a maximum of 2 W was used for the low repetition rates. For larger rates a bigger thermopile was used with a 100 W threshold and a built-in fan for refrigeration. This gave a slower response: while the small one gave a stable reading within 20 s the larger one took about 100 s. Each thermopile has a conversion factor to get a power value from the voltmeter lecture.

The photodiode was connected to an oscilloscope that shows and registers a detailed profile of the pulse power over time. For each measurement the right scales of voltage and time had to be adjusted to obtain a proper visualization of the pulse. Since the successive pulses are slightly different from each other, an automated averaging was performed to obtain a good representation on the oscilloscope screen. This image, together with the associated table of voltage-time pairs, were copied to the connected computer.

The laser comes with the software Visual Laser Marker, mostly intended for industrial marking. Its graphical interface allows creating the data file that is fed to the laser for each experiment, that, consisted in a long series of pulses focused at a single point with selected repetition rate, pulse length, pumped energy and number of pulses.

C. Performed measurements

A first set of measurements was done at the lowest pulse rate (2 kHz) to explore all the available pulse lengths (4, 8, 14, 20, 30, 50, 100 and 200 ns) and perform measurements for different pump energies at 10% increments of the maximum value All these measurements could be made with the small thermopile, but the position of the photodiode had to be adjusted between measurements a few times to avoid the saturation of the photodiode, since the power it receives increases with the pulse length. Because the photodiode detects a small part of the total power a normalization factor had to be determined for each position from the total power measured with the thermopile, the pulse power obtained by integrating the diode signal, and the repetition frequency.

Similar series of experiments were performed with pulse rates of 20 kHz and 200 kHz. In most of these measurements the beam power exceeded the threshold of the small thermopile, and the setup had to be slightly changed to place the big thermopile at approximately the same distance to the focusing lens by raising the laser, the glass and the photodiode. Due to the slower response of this thermopile, a shorter series of pulse lengths (4, 8, 30, 100 and 200 ns) was used in these sets of measurements. A series of measurements at 20 kHz, 30 ns pulse length and different pump energies were done twice, once with each thermopile to check if the results were coincident enough.

Although the laser was supposed to operate at frequencies up to 1000 kHz, the control software gave an error over 750 kHz that could not be solved (some other problems were encountered during the experiments that could be sorted out).

A CCD camera was used to get an image of the spatial profile for different configurations including pulse lengths of 4, 20, 50, 100 and 200 ns at low pump energy and an image of the beam without the lens to measure its diameter.

A last series of power measurements acquired without the glass was performed to get the true value of the output beam power.

III. RESULTS AND DISCUSSION

A. CCD camera

Fig. 4 shows a colour graded image of the spatial profile of the beam power density for a 4 ns pulse length at 2 kHz repetition rate and 5% of the maximum pump energy. These parameters lead to a laser power low enough to make possible a direct recording of the beam with the CCD camera and get an image with a well-differentiated power density distribution. This was fitted to a gaussian giving 87% of correlation, which denotes a high quality beam. Considering that there are some imperfections caused by the filters, the correlation might be even higher. Similar images were obtained under different pulse conditions.
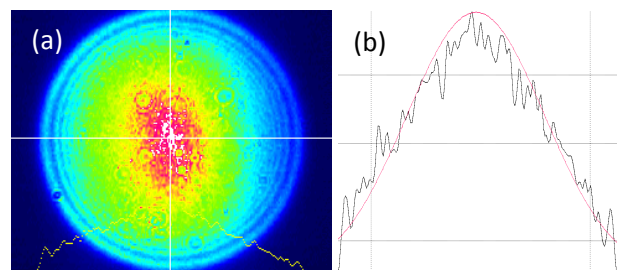

FIG. 4: (a) Colour graded image of the beam power density recorded by the CCD camera for a 4 ns pulse length at 2 kHz repetition rate and 5% of the maximum pump energy. (b) Gaussian fitting of the vertical profile.

The laser beam diameter measured without the lens was 5 mm, in good agreement with the provider specifications.

B. Thermopile

The beam power measured with the two thermopiles resulted in very similar results for all pump energies. Therefore, no reference to the thermopile used will be made from now on.

The measurements with the glass gave an 89% of those performed without it, so that all the presented results have been corrected accordingly.

Fig. 5 shows the beam power *vs* pump power at a repetition rate of 2 kHz for pulse lengths ranging from 4 ns (bottom line) to 200 ns (top line). A good linear response is obtained in all cases (*rms* > 0,99), with very small deviations appearing only at the lowest pump energies. This indicates there is a proportional relationship between the beam power and the % of pump power. For 20 and 200 kHz, higher beam powers were measured while still showing the same relation to the pumping power.
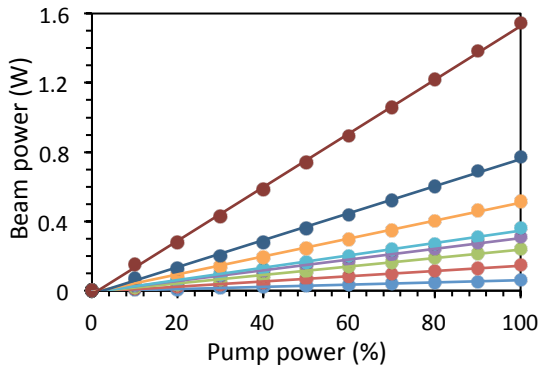
FIG. 5: Beam power *vs* pump power (% of the maximum value) at a repetition rate of 2 kHz for pulse lengths of (●) 4, (●) 8, (●) 14, (●) 20, (●)30, (●) 50, (●) 100 and (●) 200 ns.

The energy of a single pulse (E_P) was obtained by dividing the beam power (P) into the repetition rate (υ):

$$E_P = \frac{P}{\upsilon} \qquad (1)$$

Fig. 6 represents the energy per pulse *vs* pulse length at 100% pump power. The blue dots correspond to a repetition rate of 2 kHz, the red dots correspond to 20 kHz and the green ones to 200 kHz. The figure shows that the energies of pulses of the same duration but different frequency mostly coincide for 2 kHz and 20 kHz repetition rates. By raising the pulse length the pulse energy increases. Pulse energies are lower at 200 kHz, and they reach an almost constant value of 80 μJ after 8 ns pulse length. The corresponding beam power is 16 W, which is the maximum value obtained in this work. This is 16% lower that the value given in the specifications (19 W). The same power value was obtained by working at 20 kHz for 200 ns pulse length. In these conditions the pulse energy attains a maximum value of 800 μJ, again 16% lower than the value specified in the user manual (0,95 mJ).
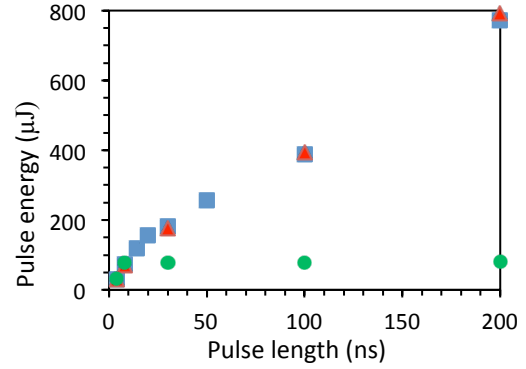
FIG. 6: Energy per pulse (eqn. (1)) *vs* pulse length at 100 % pump power. The blue (■), red (▲), and green (●) symbols correspond to pulse rates of 2 kHz, 20 kHz and 200 kHz respectively.

The fact that the energies of the pulses are nearly equal for 2 kHz and 20 kHz suggests that the time between pulses is large enough to attain the maximum population inversion. We will refer to this time as the full-charge time (t_{fc}). Therefore, $t_{fc} \leq 1/\upsilon = 50$ μs. At 200 kHz the time between pulses is 5 μs and the maximum pulse energy (80 μJ) is ten times lower than the value attained for 20 kHz, suggesting that the time needed for a full charge is in fact close to 50 μs.

The power of individual pulses (P_P) can be obtained by dividing the pulse energy E_P into the pulse length (t_P):

$$P_P = \frac{E_P}{t_P} \qquad (2)$$

Fig. 7 shows the pulse power *vs* pulse length at 100 % pump power. For a pulse rate of 200 kHz (green dots) P_P decreases as $1/t_P$ when E_P reaches its constant value (as expected). For the lower rates (red and blue dots) P_P tends to a constant value for the larger pulses. The three curves present a pronounced maximum of similar intensity for pulses of about 8 ns.
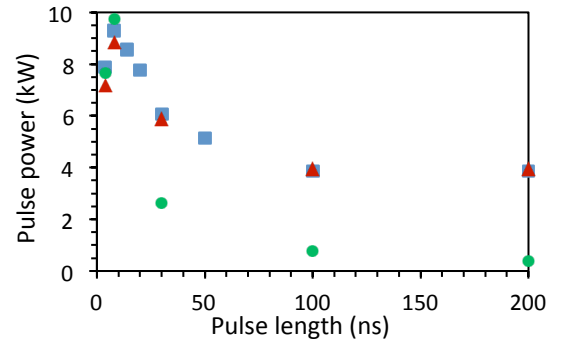
FIG. 7: Pulse power (eqn. (2)) as measured with the thermopile *vs* the pulse length at 100 % pump power. The blue (■), red (▲), and green (●) symbols correspond to pulse rates of 2 kHz, 20 kHz and 200 kHz respectively.

C. Photodiode

As for the thermopile, the photodiode gives a voltage that has to be converted to power units. Lectures were registered at time intervals of 10 ps or larger, depending on the pulse length. This instantaneous power $P(t)$ corresponds to a small fraction of the total pulse energy, which depends on the

position of the thermopile with respect to the laser beam axis. The energy of a pulse is the integral of the instantaneous power over the time lasting the pulse:

$$E_P = \int_{t_1}^{t_2} P(t)dt \qquad (3)$$

Since the collection of data is discrete this integral was calculated as a Riemann sum:

$$\sum_{i=0}^{n-1} f(t_i)(x_{i+1} - x_i) \qquad (4)$$

By comparing the result of this integral with the energy of the pulse calculated from the thermopile measurements (eqn. (1)) a coefficient was obtained that was used to convert the voltage values into total instantaneous power. The graphical representation of these values shows the actual shape of the pulses over time (Fig. 8), and gives detailed information on the pulse features, such as the peak power and its duration.
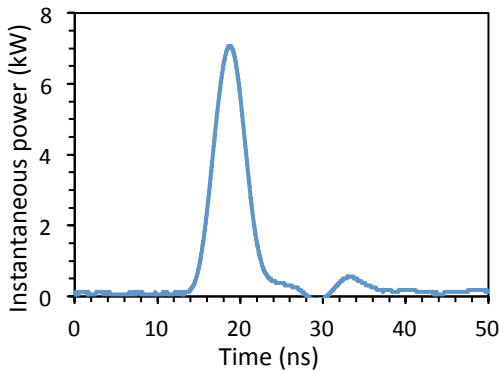

FIG. 8: Instantaneous power over duration of a 4 ns pulse for a repetition rate of 2 kHz.

Fig. 8 shows that the nominal pulse length corresponds approximately to the pulse width at half maximum. However, the shapes of longer pulses are more irregular, and this criterion is more difficult to apply. On the other hand, a pulse length can also be measured as the time at which the instant power is clearly over the background noise, which is the criterion used for integrating the signal to obtain the pulse energy. Table 1 shows these values together with the corresponding nominal lengths for 2 kHz repetition rate. Similar results were obtained for 20 kHz

Nominal	4	8	14	20	30	50	100	200
Measured	10	18	26	31	38	58	108	206

Table 1: Nominal pulse lengths and actual durations (in ns) obtained from the spatial profile for 2 kHz repetition rate.

The laser source has a Q-switching mechanism [12] for producing short pulses in the nanosecond range with peak powers over 100 times higher than the mean power of the beam. This mechanism blocks the laser effect in the interval between pulses while energy is being pumped into the gain medium (see Fig. 9). When the block is removed lasing is suddenly permitted and a burst of energy is emitted that forms the first steep slope present in most pulses, as it can be seen in Fig. 10 for different pulse lengths at 2 kHz repetition rate. Again, the results for 20 kHz are very similar.
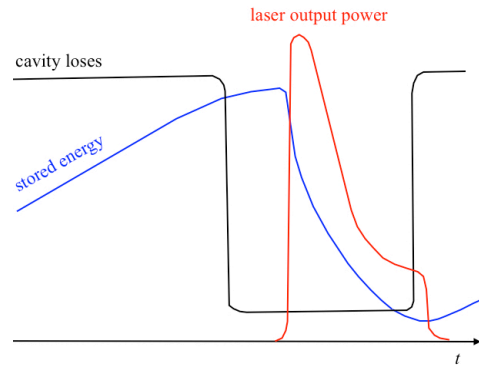

FIG. 9: Schematic representation of the pumping and the instantaneous power of a pulse in a Q-switched laser.

The pulse shape after the peak point is quite different for different pulse lengths. For all but the shortest pulse an inflection point appears in the decreasing part of the curve, and the instant power almost stabilizes at somewhat less than half the peak power until the pulse is forced to end by the Q-switch. No clear inflection point is observed in the 200 ns pulse shape, that shows a gradually decreasing slope. No satisfactory explanation has been found for those different shapes, that differ from the results derived in a previous work on Q-switch theoretical modelling [12].
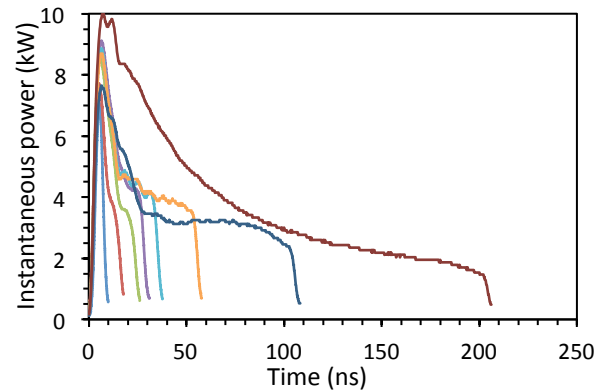

FIG. 10: Instantaneous power over time for pulses of lengths from 4 to 200 ns at 2 kHz repetition rate and 100% pump power. The shortest one being 4 ns and the longest 200 ns.

The peak power of the pulses obtained from Fig.10 vary from 7 to 10 kW, the highest value corresponding to the 200 ns pulse. This coincides with the value given by the provider.

For different pumping energies the shape remains mostly the same. With regard to the effect of the frequency, the pulse shapes for 20 kHz are very similar to those shown for 2 kHz, as previously found for other laser properties, but the shapes change significantly for 200 kHz, as shown in Fig. 11 for the 100 and 200 ns pulses. The 100 ns pulse starts with the same initial burst and starts the downslope that is observable in other pulses, but it doesn't stabilize after that and increases its power again to reach the maximum power at the final part of the pulse. The 200 kHz 200 ns pulse has the lowest average power and is the only one that doesn't present a clear initial power burst followed by a decrease, instead its power is approximately constant along the pulse duration, reaching a maximum near the middle. The effect of the frequency on the pulse shape is probably related to the fact that, as previously shown, only a tenth part of the population inversion is

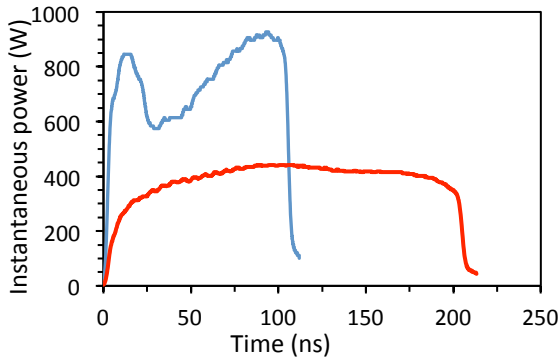reached at 200 kHz in comparison to 2 and 20 kHz, which greatly affects the instantaneous power and the shape.

FIG. 11: Instantaneous power over the duration of a 100 (blue) and a 200 ns (red) pulse for a repetition rate of 200 kHz.

IV. CONCLUSIONS

- The laser beam diameter measured is 5mm, in good agreement with the manufacturer specifications, and has a gaussian spatial distribution.
- The maximum beam power is 16 W, 16% lower than the value given by the manufacturer.
- The beam power shows a good linear correlation with the pump power for all available pulse lengths and repetition rates.

- The energy per pulse increases monotonically with the pulse length for 2 and 20 kHz repetition rates, but a maximum of 80 µJ is attained after 8 ns pulse length for 200 kHz. The pulse energy at 20 kHz and 200 ns is 800 µJ, 16% less than the specifications.
- The time needed for attaining the maximum population inversion is about 50 µs.
- The pulse power *vs* pulse length presents a pronounced maximum at ≈8 ns of similar intensity for 2, 20 and 200 kHz repetition rates. The maximum peak power obtained is 10 kW
- The time shape of the pulses is strongly dependent on the pulse length. Similar shapes result for 2 and 20 kHz, and these are quite different to those obtained for 200 kHz, probably due to the low population inversion attained in the latter case.
- It has been found that the laser doesn't work at pulse repetitions rates over 750 kHz.

[1] T. H. Maiman, «Stimulated optical radiation in ruby», *Nature*, vol. 187, pp. 493-494, 1960.

[2] E. Snitzer, «Optical maser action of Nd^{3+} in a barium crown glass», *Physical Review*, vol. 7, pp. 444-446, 1961.

[3] E. Snitzer, «Proposed fiber cavities for optical masers», *Journal of Applied Physics*, vol. 32, pp. 36-39, 1961.

[4] Ch. J. Koester and E. Snitzer, «Amplification in a fiber laser», *Applied Optics*, vol. 3, pp. 1182-1186, 1964.

[5] Valeri (Vartan) Ter-Mikirtychev, «Fundamentals of fiber lasers and fiber amplifiers», Heidelberg: Springer, 2014.

[6] Michel J. F. Digonnet, ed., «Rare-Earth-Doped Fiber Lasers and Amplifiers». Second Edition, Revised and Expanded, New York: Marcel Dekker, Inc., 2001.

[7] D. J. Richardson, J. Nilsson, and W. A. Clarkson, «High power fiber lasers: current status and future perspectives», *Journal of the Optical Society of America B*, vol. 27, pp. B63-B92, 2010.

[8] «Rofin Fiber Lasers. PowerLine F Series for Marking and Micro Processing», https://www.rofin.com/en/products/fiber-lasers/powerline-f/powerline-f-203050100/[Accessed on 18/5/19]

[9] H. M. Pask, R. J. Carman, D. C. Hanna, A. C. Tropper, C. J. Mackechnie, P. R. Barber and J. M. Dawes, «Ytterbium-Doped Silica Fiber Lasers: Versatile Sources for the 1-1.2 µm Region», IEEE *Journal of Selected Topics in Quantum Electronics*, vol. 1, pp. 2-13, 1995.

[10] J. O. White, « Parameters for Quantitative Comparison of Two-, Three-, and Four-Level Laser Media, Operating Wavelengths, and Temperatures», *The IEEE Journal of Quantum Electronics,* vol. 45, pp. 1213-1220, 2009.

[11] «PowerLine F. Assembly and Operating Instructions» ver 3.3, Coheren Rofin.

[12] J. Liu, D. Shen, S. C. Tam and Y. L. Lam, «Modeling Pulse Shape of Q-Switched Lasers», *The IEEE Journal of Quantum Electronics,* vol. 37, pp. 888-896, 2001.